Malaysian Journal of Civil Engineering 27(2):204-222 (2015)

NUMERICAL EVALUATION OF UNSATURATED FLOW IN POROUS MEDIA USING ITERATIVE TECHNIQUES FOR VARIOUS SOILS

M. Sayful Islam

Department of Mathematics, Shahjalal University of Science & Technology, Sylhet-3114, Bangladesh

Corresponding Author: sislam_25@yahoo.com*

Abstract: Unrelenting difficulties that arise in forming numerical solutions of water flow in variably saturated problems include controlling the stability of the nonlinear equation solver. Besides, the accuracy of solutions, also of concern is the required computational effort, especially when nonlinear soil hydraulic properties and dry initial conditions are involved. A general numerical algorithm in the context of finite element formulation and Picard and Newton iteration schemes are described to solve Richards' equation, in which a mass-conservative, head based formulation is proposed to approximate the governing equation, and mass-lumping techniques is employed to improve solution convergence and stability behavior. A difficult one-dimensional test case presented emphasizes different aspects of the performance of the iterative methods and the different issues that can influence their convergence and efficiency. The result is validated with extensive average values of soil hydraulic parameters for 12 soil textural groups.

Keywords: *Saturation, numerical solution, finite element, iterative techniques, Picard and Newton schemes*

1.0 Introduction

The parabolic partial differential equation describing fluid flow in partially saturated porous media, Richards' equation, is obtained by combining Darcy's law with the continuity equation, assuming that air effects and compressibility of both water and the solid matrix are negligible which is highly nonlinear due to pressure head dependencies in the specific soil moisture capacity and relative hydraulic conductivity terms**.**

Numerical solution of saturated-unsaturated flows is widely used in many branches of science and engineering including agricultural engineering, ground water engineering, chemical contaminants tracing, and rainfall-runoff modeling. Numerical solutions of the Richards' equation via the finite-element and finite-difference techniques readily exist. Finite-elements have been successfully used to solve the general variably saturated flow equation by several researchers [Cooley, 1983; Huyakorn *et al*., 1984, 1986; Neuman,

1973]. However, all of these finite-element models are pressure-based, finite difference, Euler time marching algorithms to approximate the transient term, which can produce high mass-balance errors. Latest advances are discussed in finite-element modeling techniques for variably saturated flow problems.

In the numerical modeling of variably saturated flow, it is important to combine the solution accuracy with realistic computing time. To linearize the highly nonlinear governing Richards' equation usually necessitates the use of Picard and Newton iterative scheme. Theoretically, the Newton method converges one order faster than the Picard method, but under some situations, the Picard method is more efficient than the Newton method [Paniconi and Putti, 1994]. The Newton method converges quardatically only in the vicinity of the solution. When the approximated values used to form the Jacobian matrix is not close to the solution, this technique gives increase to rigorous non-physical oscillation in the iteration, and diverge consequently because high order terms are neglected in the Taylor series expansion, which contribute to the right-hand side vector of the linear system, are still significant and the Jacobian matrix is devoid of diagonal dominance.

The Picard method has a diagonally dominant matrix, but still gives rise to the iteration-to-iteration oscillation that causes divergence. An important factor that affects the convergence of the Picard method is the gravity term as it is treated, in analogy with the time step advance technique, explicitly in the iteration, whilst a robust method requires implicit approach. An improvement in the convergence is related to an improvement in stability. For example, some common approaches such as the reduction of time step, the use of under relaxation and the mass lumped technique are methods to improve the stability by enhancing the diagonal terms of the matrix of the linear system [Neuman, 1973]. Several methods e.g., line search methods [Pan and Wierenga, 1997; Williams *et al*., 2000] are available for searching the optimal relaxation factors, but they are expensive. The use of small time steps for convergence is time consuming.

The present paper develop and present a computationally simple procedure for solution of nonlinear equation systems resulting from finite element solutions of variably saturated flow problem, which is accurate and efficient and have been reliable for all tested thus far. The finite element scheme used is the subdomain method, and although relatively standard. Choice of finite element scheme over simpler finite difference schemes is based on stability of the resulting nonlinear equation system.

2.0 Numerical Procedures

2.1 Governing Equation

For one-dimensional vertical flow of water in a variably saturated rigid soil under isothermal condition, Richards' equation is written as

$$S(\psi)\frac{\partial \psi}{\partial t} = \frac{\partial}{\partial z}\left(K(\psi)\left(\frac{\partial \psi}{\partial z} + 1\right)\right) \quad (1)$$

where, ψ is the pressure head [L], t is time [T], z denotes the vertical distance from the soil surface downward [L], K(ψ) is the hydraulic conductivity [LT^{-1}], $S(\psi) = \frac{d\theta}{d\psi} + \left(\frac{\theta}{\phi}\right)S_s$ is the general storage term, θ is the volumetric water content, $\frac{d\theta}{d\psi}$ is the specific soil moisture capacity [L^{-1}], ϕ is porosity, S_s is specific storage.

2.2 Equations for Soil Hydraulic Properties

Numerical solution of Richards' equation needs to specify the constitutive relations between the dependent variable (pressure head) and the nonlinear terms (moisture content, moisture capacity, and conductivity). These characteristic retention functions can be input to a numerical model as data in tabular form, or, more frequently, as experimental expression fitted to observed data. Separate expression of relation between moisture capacity and pressure head is not required because this relation will follow by differentiating the moisture content-pressure head task. Conductivity-pressure head function obtained from the moisture content-pressure head function, using some physically based approach such as the distribution of pore sizes, is commonly used. In this technique the quantity of fitting factors in the characteristic soil relations is kept to a least, and the need for unsaturated conductivity measurements is precluded, permitting the relations to be fitted using only measurements of moisture content, saturated hydraulic conductivity, and pressure head, which are more easily obtained and more consistent.

The soil characteristic equations used in the work reported here are given by van Genuchten and Nielsen model [van Genuchten and Nielsen, 1985].

$$\theta(\psi) = \theta_r + \frac{\theta_s - \theta_r}{[1+|\alpha\psi|^n]^m} \quad \text{if } \psi \leq 0 \quad (2a)$$

$$\theta(\psi) = \theta_s \quad \text{if } \psi > 0 \quad (2b)$$

$$K(\psi) = K_s \left[\frac{\theta-\theta_r}{\theta_s-\theta_r}\right]^{\frac{1}{2}} \left\{1 - \left[1 - \left(\frac{\theta-\theta_r}{\theta_s-\theta_r}\right)^{\frac{1}{m}}\right]^{m}\right\}^2 \quad \text{if } \psi \leq 0 \quad (3a)$$

$$K(\psi) = K_s \quad \text{if } \psi > 0 \quad (3b)$$

$$c(\psi) = \alpha m n \frac{\theta_s-\theta_r}{[1+|\alpha\psi|^n]^{m+1}} |\alpha\psi|^{n-1} \quad \text{if } \psi \leq 0 \quad (4a)$$

$$c(\psi) = 0 \quad \text{if } \psi > 0 \quad (4b)$$

where, θ_r is the residual moisture content, θ_s is the saturated moisture content, $m = 1 - \frac{1}{n}$, and *n* and α are fitting parameters.

2.3 Finite Element Models

For the numerical solution of Richards' equation (1), in this study use a finite element Galerkin discretization in space and a finite difference first order backward Euler scheme in the time derivative term.

To develop the finite element model, the problem domain is discretized into *M-1* elements defining *M* global nodes and let the pressure head function ψ be approximated by a trial function of the form:

$$\psi(z,t) \approx \hat{\psi}(z,t) = \sum_{J=1}^{M} N_J(z)\psi_J(t) \quad (5)$$

where $N_J(z)$ and $\psi_J(t)$ are linear Lagrange basis functions and nodal values of ψ at time *t*, respectively, *M* is the number of nodes in the finite element network. The method of weighted residuals is used to set the criteria to solve for the unknown coefficients. In local coordinate space $-1 \leq \xi \leq 1$, the approximating function for each element (e) is $\hat{\psi}^{(e)} = \sum_{i=1}^{2} N_i^{(e)}(\xi)\,\psi_i^{(e)}(t) = \frac{1}{2}(1-\xi)\psi_1^{(e)}(t) + \frac{1}{2}(1+\xi)\psi_2^{(e)}(t)$ which we can write in vector form as $\hat{\psi}^{(e)} = \left(\boldsymbol{N}^{(e)}(\xi)\right)^T \boldsymbol{\Psi}^{(e)}(t)$. The global function (5) becomes

$$\hat{\psi} = \sum_{e=1}^{M-1} (\boldsymbol{N}^{(e)})^T \boldsymbol{\Psi}^{(e)} = \sum_{e=1}^{M-1} \hat{\psi}^{(e)} \quad (6)$$

The symmetric weak formulation of Galerkin's method applied to (1) yields the system of ordinary differential equations [Paniconi *et al*., 1991]:

$$\boldsymbol{A}(\boldsymbol{\Psi})\boldsymbol{\Psi} + \mathbf{F}(\boldsymbol{\Psi})\frac{\mathrm{d}\boldsymbol{\Psi}}{\mathrm{dt}} = \mathbf{q}(\mathrm{t}) - \mathbf{b}(\boldsymbol{\Psi}) \quad (7)$$

where $\boldsymbol{\Psi}$ is the vector of undetermined coefficients corresponding to the values of pressure head at each node, $\boldsymbol{q}$ contains the specified Darcy flux boundary conditions, and $\boldsymbol{A}$, $\boldsymbol{b}$, and $\boldsymbol{F}$ are given over local subdomain element $\boldsymbol{\Omega}^{(e)}$ as

$$\boldsymbol{A}^{(e)} = \int_{\boldsymbol{\Omega}^{(e)}} \boldsymbol{K}_s^{(e)} K_r(\hat{\psi}^{(e)}) \frac{\boldsymbol{dN}^{(e)}}{\boldsymbol{dz}} (\frac{\boldsymbol{dN}^{(e)}}{\boldsymbol{dz}})^T dz \quad (8)$$

$$\boldsymbol{b}^{(e)} = \int_{\boldsymbol{\Omega}^{(e)}} \boldsymbol{K}_s^{(e)} K_r(\hat{\psi}^{(e)}) \frac{\boldsymbol{dN}^{(e)}}{\boldsymbol{dz}} dz \quad (9)$$

$$\boldsymbol{F}^{(e)} = \int_{\boldsymbol{\Omega}^{(e)}} S(\hat{\psi}^{(e)})\, \boldsymbol{N}^{(e)} (\boldsymbol{N}^{(e)})^T dz \quad (10)$$

Here $\boldsymbol{N}^T$ to denote the transpose of $\boldsymbol{N}$.

Second order Gaussian quadrature formula is employed for estimating the nonlinear integrals in (8), (9), and (10) introducing an additional source of numerical error. The magnitude of this error will depend on the degree of nonlinearity in the $K_r(\psi)$ and $S(\psi)$ characteristic equations and can be minimized by using higher order numerical quadrature or a smaller mesh size Δz [Pan and Wierenga, 1997].

2.4 Time Differencing

A λ-weighted finite difference discretization (Crank-Nicolson when λ =0.5, backward Euler when λ =1) is used in the time derivative term of (7), with super scrip *k* denoting time step, we get

$$\boldsymbol{A}\left(\boldsymbol{\Psi}^{k+\lambda}\right)\boldsymbol{\Psi}^{k+\lambda} + \boldsymbol{F}\left(\boldsymbol{\Psi}^{k+\lambda}\right)\frac{\boldsymbol{\Psi}^{k+1}-\boldsymbol{\Psi}^{k}}{\Delta t} = \boldsymbol{q}\left(t^{k+\lambda}\right) - \boldsymbol{b}(\boldsymbol{\Psi}^{k+\lambda}) \quad (11)$$

where $\boldsymbol{\Psi}^{k+\lambda} = \boldsymbol{\lambda}\boldsymbol{\Psi}^{k+1} + (1-\lambda)\boldsymbol{\Psi}^{k}$; $0 \le \lambda \le 1$ (12)

The system of equations (11) is nonlinear in $\boldsymbol{\Psi}^{k+1}$ except when $\lambda = 0$, which corresponds to the explicit Euler scheme. In the implicit case ($\lambda > 0$), some iteration or linearization strategy is required to solve the system of equations. In selecting a linearization strategy to solve a nonlinear equation such as (11), it seems most reasonable to choose a method which has truncation error of the same order as the

accuracy of the discretization scheme, since the accuracy of the overall numerical algorithm will be that of its component scheme with the lowest order of accuracy.

3.0 Iterative Methods

3.1 Newton Scheme

Let us consider

$$\boldsymbol{f}\left(\boldsymbol{\Psi}^{k+1}\right) = \boldsymbol{A}\left(\boldsymbol{\Psi}^{k+\lambda}\right)\boldsymbol{\Psi}^{k+\lambda} + \boldsymbol{F}\left(\boldsymbol{\Psi}^{k+\lambda}\right)\frac{\boldsymbol{\Psi}^{k+1}-\boldsymbol{\Psi}^{k}}{\Delta t} - \boldsymbol{q}\left(t^{k+\lambda}\right) - \boldsymbol{b}\left(\boldsymbol{\Psi}^{k+\lambda}\right) = 0 \quad (13)$$

Letting superscript *m* be an iteration index, the Newton scheme [Paniconi *et al*., 1991] is

$$\boldsymbol{f}'\left(\boldsymbol{\Psi}^{k+1,\ m}\right)\boldsymbol{h} = -\boldsymbol{f}\left(\boldsymbol{\Psi}^{k+1,\ m}\right) \quad (14)$$

where $\boldsymbol{h} = \boldsymbol{\Psi}^{k+\lambda,\ m+1} - \boldsymbol{\Psi}^{k+\lambda,\ m}$ (15)

and

$$f_{ij}^{'} = \lambda A_{ij} + \frac{1}{\Delta t^{k+1}}F_{ij} + \sum_s \frac{\partial A_{is}}{\partial \psi_j^{k+1}}\psi_s^{k+\lambda} + \frac{1}{\Delta t^{k+1}}\sum_s \frac{\partial F_{is}}{\partial \psi_j^{k+1}}\left(\psi_s^{k+1} - \psi_s^{k}\right) + \frac{\partial b_i}{\partial \psi_j^{k+1}} \quad (16)$$

is the *ij*th component of the Jacobian matrix $\boldsymbol{f}'\left(\boldsymbol{\Psi}^{k+1}\right)$.

3.2 Picard Scheme

The Picard scheme [9] has simple formulation which can be obtained directly from (11) by iterating with all linear occurrences of $\boldsymbol{\Psi}^{k+1}$taken at the current iteration level *m+1* and all nonlinear occurrences at the previous level *m*. We get,

$$\left[\lambda\boldsymbol{A}\left(\boldsymbol{\lambda\Psi}^{k+\lambda,\ m}\right) + \frac{1}{\Delta t}\boldsymbol{F}\left(\boldsymbol{\Psi}^{k+\lambda,\ m}\right)\right]\boldsymbol{h} = -\boldsymbol{f}\left(\boldsymbol{\Psi}^{k+1,\ m}\right) \quad (17)$$

3.3 Convergence Criterion

Dynamic time stepping control is used to adjust step size of time during simulation according to the convergence behavior of the nonlinear iteration scheme. For each time step, a convergence tolerance ($tol=10^{-3}$) is specified, along with a maximum number of iterations, *maxit (=10*). The simulation begins with a time step size of Δt_0 and proceeds until time $T_{max}(= 17280\ s)$. The current time step size is increased by a factor of

Δt_{mag} (= 1.20) to a maximum size of $\Delta t_{max} = 10^3 s$ if convergence is achieved in fewer than $maxit_1$ (= 5) iterations, it is remain unchanged if convergence required between $maxit_1$ and $maxit_2$ (= 8) iterations, and it is decreased by a factor of Δt_{red}(= 0.5) to a minimum of Δt_{min}(= $10^{-6} s$) if convergence required more than $maxit_2$ iterations. If convergence is not achieved within *maxit*, the solution at the current time level is recomputed using a reduced time step size to the minimum time step size Δt_{min}. For the first time step of simulation, the initial conditions are used as the first solution estimate for the iterative procedure. For subsequent time steps of simulation the pressure head solution from the previous step is used as the first estimate. Thus time step size has a direct effect on convergence behavior, via its influence on the quality of the initial solution estimate. Back-stepping is also triggered if linear solver failed or if the convergence or residual errors become larger than maximum allowable convergence or residual error in the nonlinear solution. BiCGSTAB, bi-conjugate gradients stabilized method with the tolerance 10^{-10} is used to solve the generated system of linear equations and maximum iteration is 1000. For the nonlinear iterative methods, the infinity norm (l_∞) of the convergence error is used as the termination criterion; that is, when $\left\|\boldsymbol{\Psi}^{k+\lambda,\ m+1} - \boldsymbol{\Psi}^{k+\lambda,\ m}\right\| \leq tol$ is satisfied, convergence is achieved. [10]. The residual error ($\left\|\boldsymbol{f}\left(\boldsymbol{\Psi}^{k+1,\ m}\right)\right\|$) is computed using l_∞ and l_2 norms.

4.0 Numerical Simulations

The behavior of the soil hydraulic functions on simulated pressure head by numerically simulated infiltrating into an initially unsaturated homogeneous soil column. Results are obtained with CATHY (CATchment HYdrology) model that features elements of both the sequential noniterative and sequential iterative coupling schemes. CATHY is a physically-based hydrological model where the surface module resolves the one-dimensional (1D) diffusion wave equation and the subsurface module solves the 3D Richards equation. Coupling between these two equations is based on an extension of the boundary condition switching procedure used in some subsurface models for the handling of atmospheric inputs on the land surface boundary of the catchment. The main objective of this work is to assess, via sensitivity analysis, the accuracy, computational effort and mass balance limitations for the CATHY model over 12-groups of soil hydraulic parameters which make soil retention functions are highly nonlinear.

In this study, considered infiltration in a 100 cm long soil column that initially was assumed to be in equilibrium with an imposed pressure head of -1000 cm at the bottom of the column and a zero pressure head at the top of the column. Calculations were performed using nodal spacing of 1 cm, depending upon the nonlinearity of the simulated problem. Simulations were carried out for the soil hydraulic data listed in Table 1 which is obtained from Carsel and Parrish [Carsel and Parrish, 1988]..

Table 1: Average values of soil hydraulic parameters for 12 soil textural groups according to Carsel and Parrish [11]

	Texture	θ_r	θ_s	$\alpha\ (cm^{-1})$	n	$K_s\ (cm/day)$
Soil-1	Sand	0.045	0.430	0.145	2.68	712.80
Soil-2	Loamy sand	0.057	0.410	0.124	2.28	350.20
Soil-3	Sandy loam	0.065	0.410	0.075	1.89	106.10
Soil-4	Loam	0.078	0.430	0.036	1.56	24.96
Soil-5	Silt	0.034	0.460	0.016	1.37	6.00
Soil-6	Silt loam	0.067	0.450	0.020	1.41	10.80
Soil-7	Sandy clay loam	0.100	0.390	0.059	1.48	31.44
Soil-8	Clay loam	0.095	0.410	0.019	1.31	6.24
Soil-9	Silty clay loam	0.089	0.430	0.010	1.23	1.68
Soil-10	Sandy clay	0.100	0.380	0.027	1.23	2.88
Soil-11	Silty clay	0.070	0.360	0.005	1.09	0.48
Soil-12	Clay	0.068	0.380	0.008	1.09	4.80

The computed pressure head profiles for soils 1-11 are displayed in Figure 1(Soil-1 to Soil-6) and Figure 2 (Soil-7 to Soil-11). The result for the case of Soil-12, very poor performance was obtained for both the Picard and Newton schemes. None of the Newton and Picard runs converged, although a very small time step size ($\Delta t_{min} = 10^{-10}\ s$) was needed. These solutions are very similar to those reported in the literature [Celia, 1990; Vogel, 2001]. Notice that, little differences between Picard and Newton schemes are shown for the case of Soil-7.

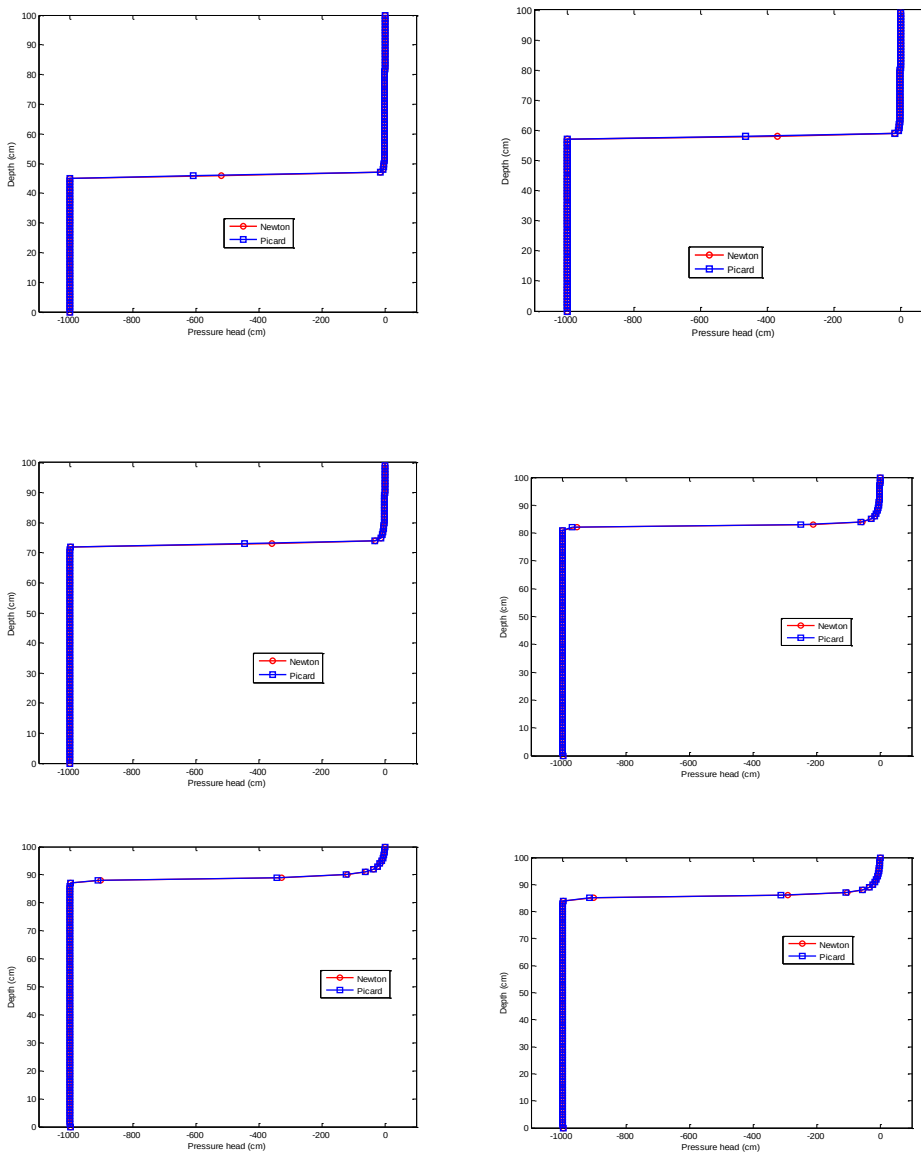

Figure 1: Computed pressure head profiles of Soil-1 to Soil-6 respectively

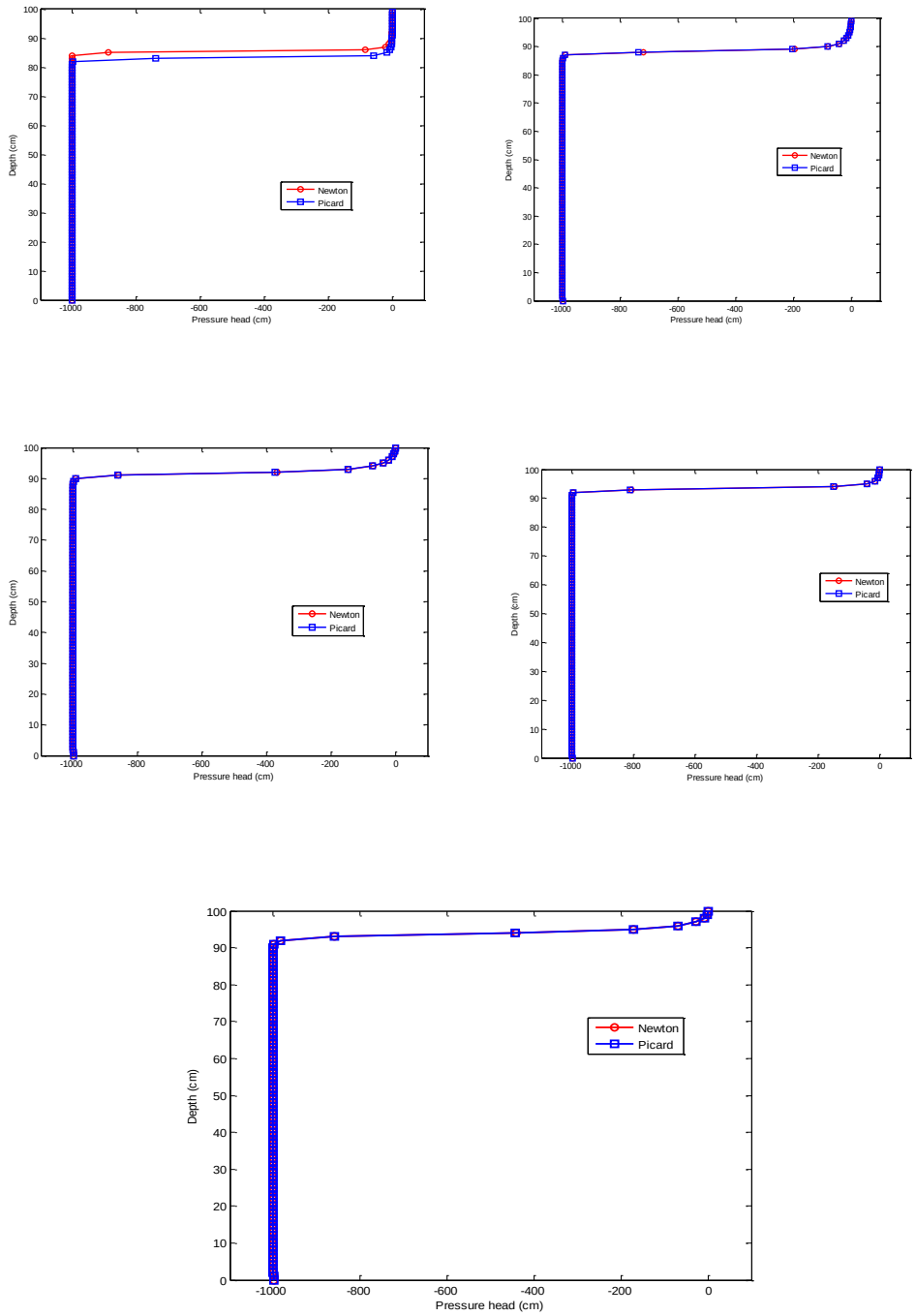

Figure 2: Computed pressure head profiles of Soil-7 to Soil-11respectively.

In the investigation of solution behavior, adaptive time stepping behavior (Figure 3 and Figure 4) of Picard and Newton techniques for all soil hydraulic parameters are included. It is found that most striking here almost similar behavior for all soils of Picard and Newton scheme during the simulation. Time step size is increased repeatedly for both the iterative schemes. During simulation in the problem domain, Picard scheme is dominated than Newton scheme for all the cases. Also, note that Picard and Newton schemes never achieved allowable maximum time step size.

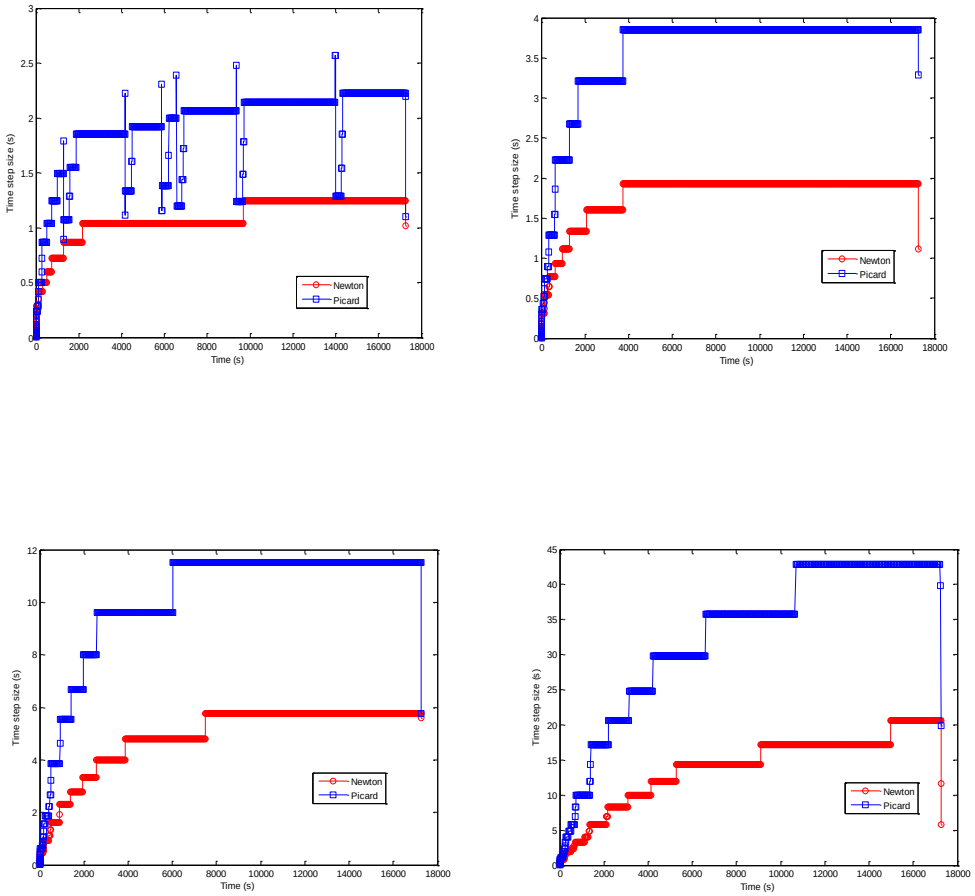

Figure 3: Time stepping behavior of Soil-1 to Soil-4 respectively.

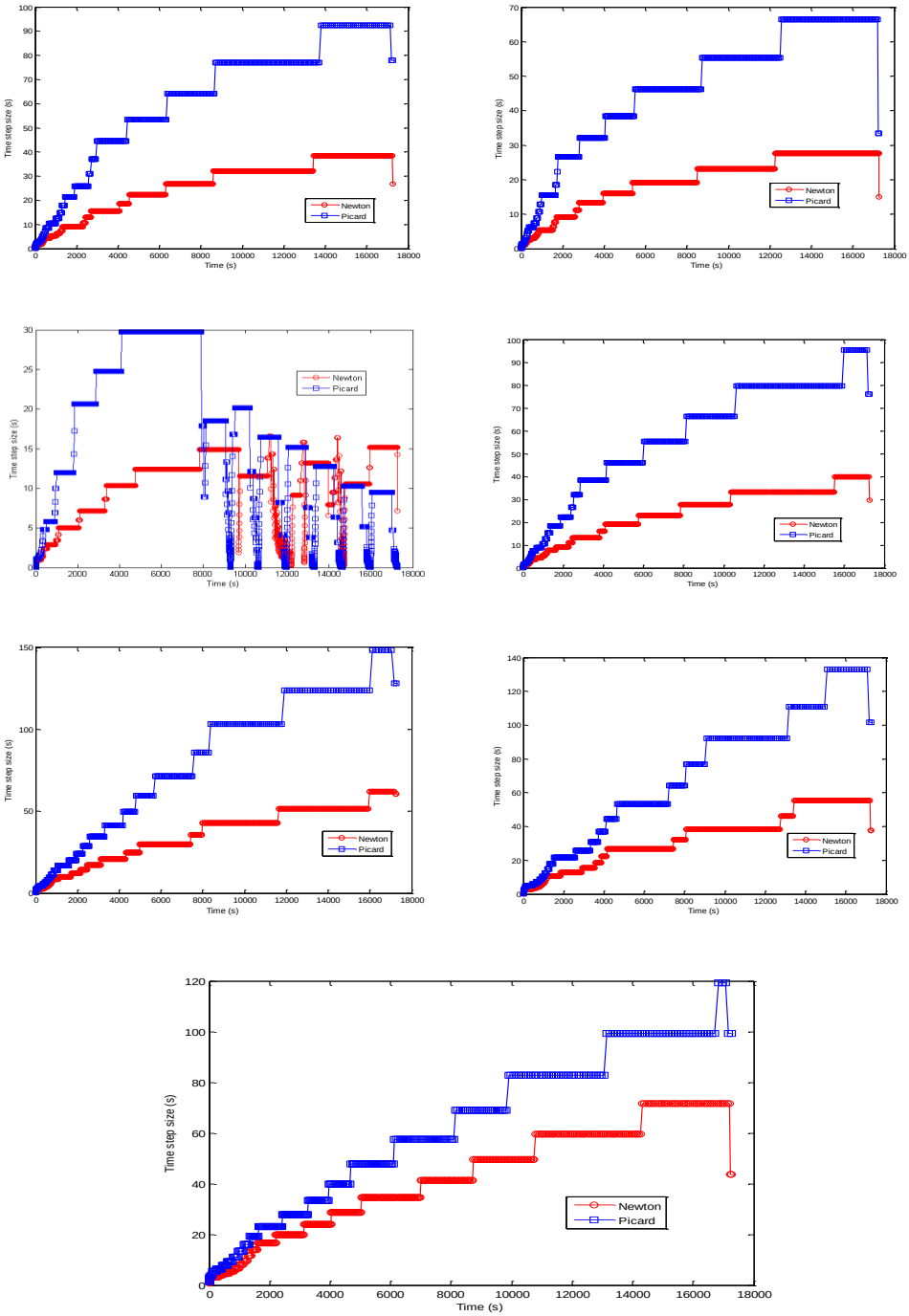

Figure 4: Time stepping behavior of Soil-5 to Soil-11 respectively.

Figure 5 and Figure 6 are graphical representation of the convergence behavior of the Picard and Newton schemes in terms of the number of nonlinear iterations required at each time step. Both techniques are needed almost 4 to 7 iterations to complete the simulation except for the case of soil 7. Constants convergence oscillations are shown in the simulation of soil-7.

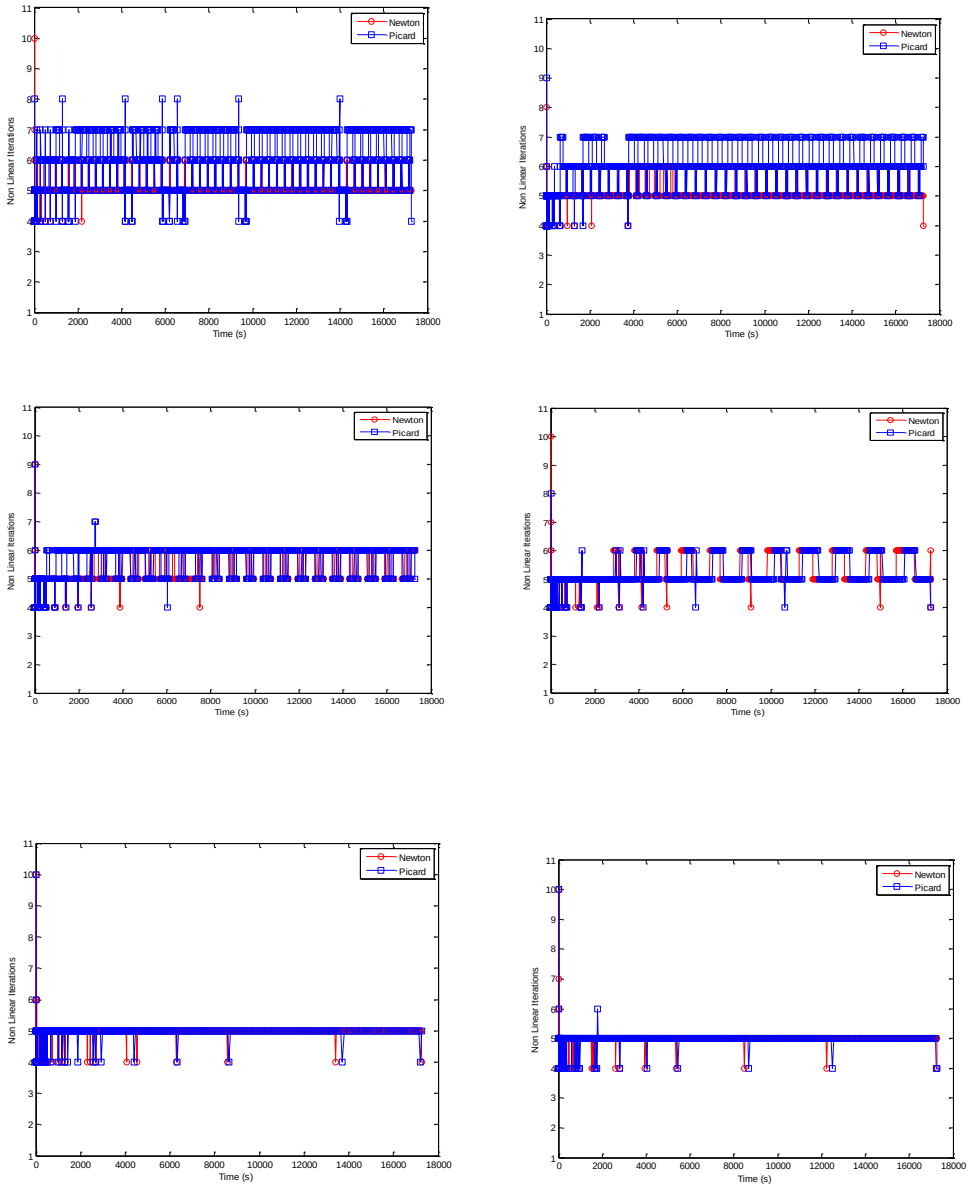

Figure 5: Convergence behavior for all Soil-1 to Soil-6 respectively.

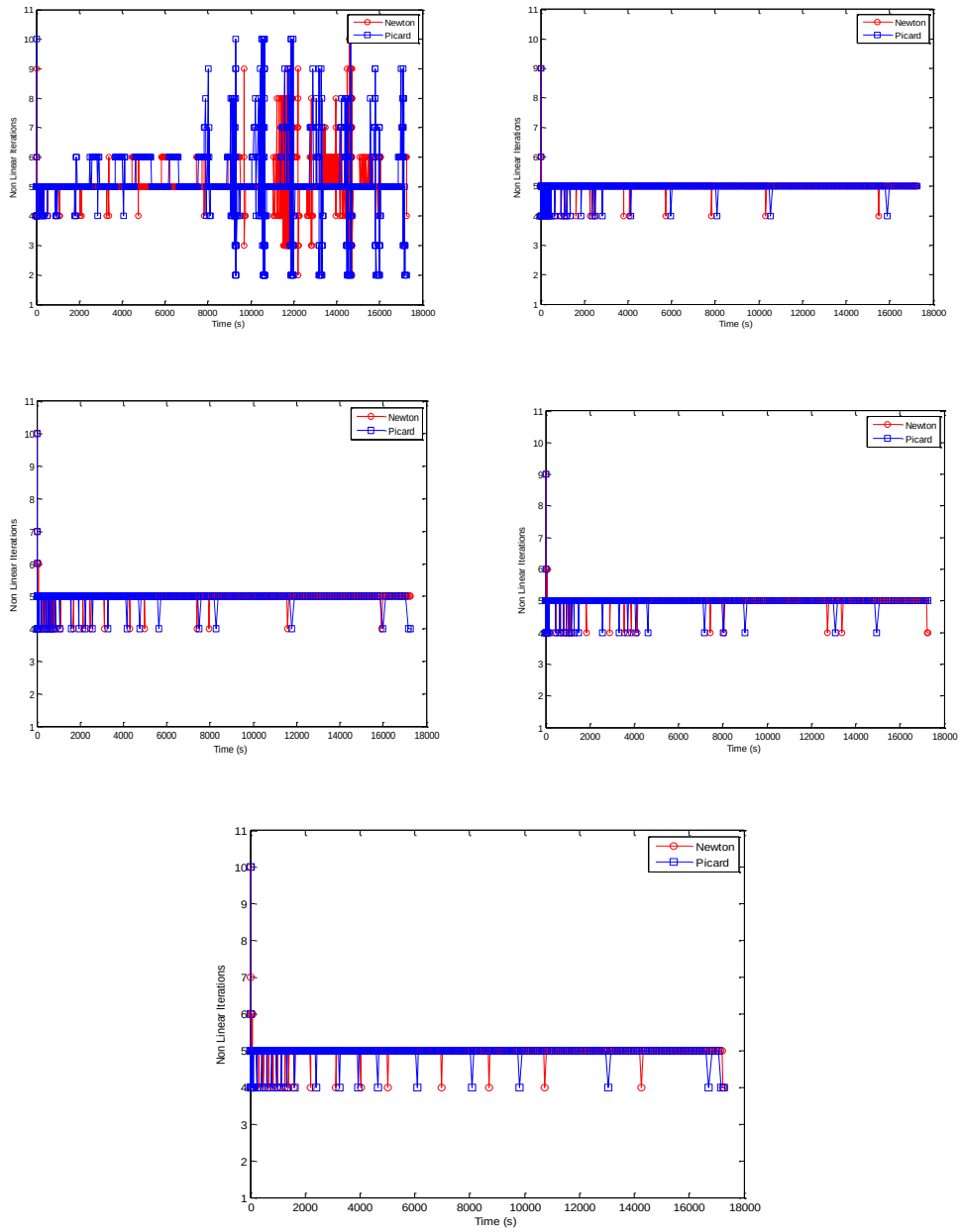

Figure 6: Convergence behavior for all Soil-7 to Soil-11 respectively.

The cumulative mass balance errors plots are shown in Figure 7 and Figure 8 for Picard and Newton schemes of Soil-1 to Soil-11. Excellent mass balance errors are shown for all the cases. This implies the numerical results are strictly maintained accuracy.

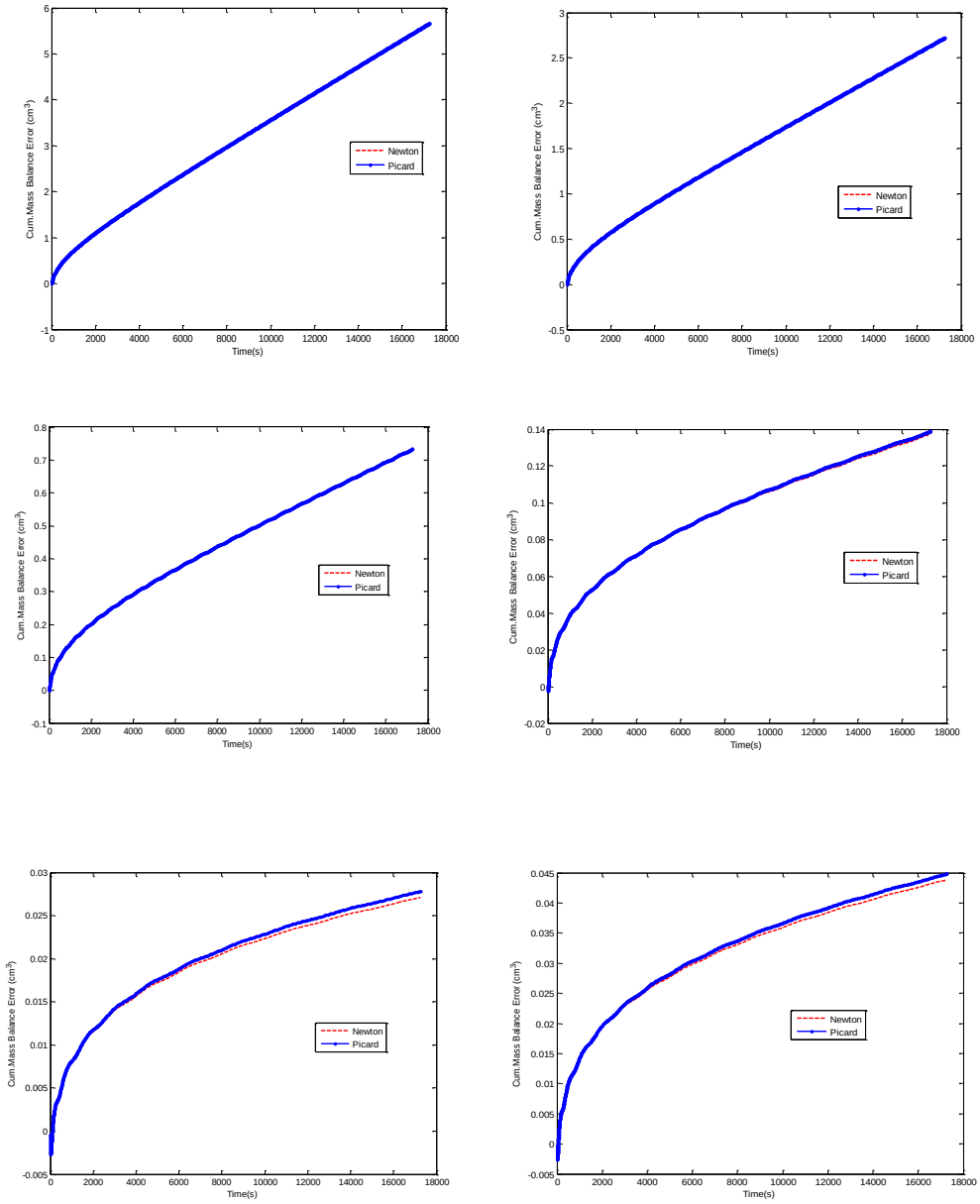

Figure 7: Cumulative mass balance error behavior for Soil-1 to Soil-6 respectively

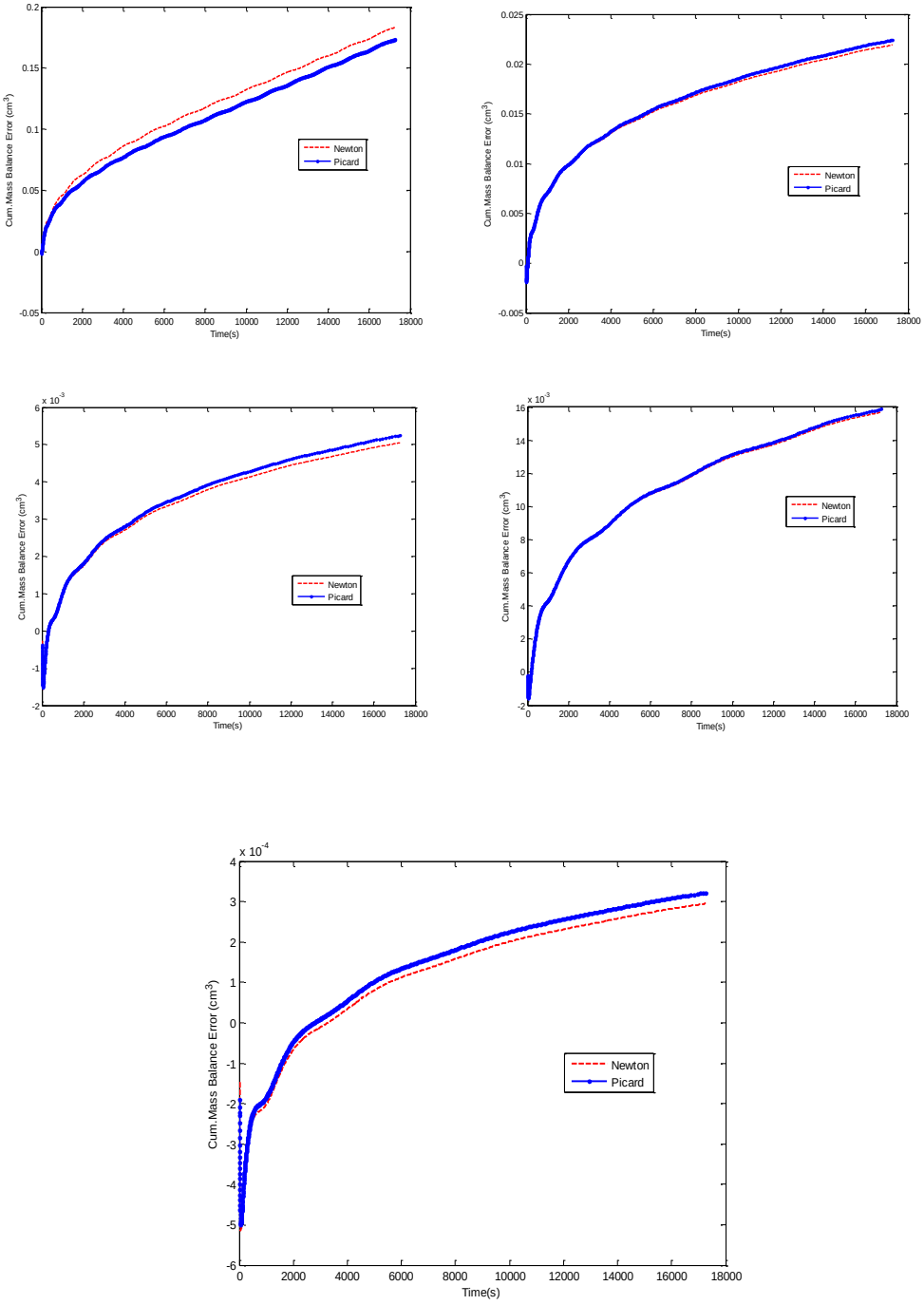

Figure 8: Cumulative mass balance error behavior for Soil-7 to Soil-11 respectively.

Summary statistics for the Picard and Newton schemes for all soil parameters are presented in Table 2 and Table 3. There are different performance indicators such as: total volumetric mass balance error, total number of time steps, largest, smallest and average step size, the average number of Picard and Newton iterations taken at each time step, the average number of iterations needed to solve the linear algebraic system at each nonlinear iterations and CPU. From the CPU column, observed that the Newton scheme is computationally less efficient than the Picard scheme for all the case. Computational results shown the theoretically expected rates of convergence are achieved. Also, it is clear that both the schemes to be stable for all soil hydraulic parameters except for Soil-12.

Table 2: Computational statistics of the CATHY model for Newton and Picard schemes

Texture	Scheme	MBE (cm^3)	No. of Time steps	Largest time step size	Smallest time step size	Avg. Time step size
Soil-1	Newton	5.667e+0	17058	1.242e+0	1.192e-6	1.013e+0
	Picard	5.667e+0	10191	2.571e+0	1.192e-6	1.696e+0
Soil-2	Newton	2.723e+0	10737	1.926e+0	9.537e-6	1.609e+0
	Picard	2.723e+0	5597	3.851e+0	1.907e-5	3.087e+0
Soil-3	Newton	7.320e-1	4499	5.759e+0	3.052e-4	3.841e+0
	Picard	7.333e-1	2231	1.152e+1	6.104e-4	7.745e+0
Soil-4	Newton	1.373e-1	1986	2.067e+1	8.766e-3	8.701e+0
	Picard	1.389e-1	912	4.286e+1	9.766e-3	1.895e+1
Soil-5	Newton	2.709e-2	1168	3.845e+1	7.813e-2	1.479e+1
	Picard	2.781e-2	550	9.229e+1	1.563e-1	3.142e+1
Soil-6	Newton	4.382e-2	1472	2.769e+1	3.906e-2	1.174e+1
	Picard	4.481e-2	675	6.645e+1	7.183e-2	2.560e+1
Soil-7	Newton	1.831e-1	2619	1.659e+1	4.883e-3	6.598e+0
	Picard	1.734e-1	7745	2.976e+1	9.766e-3	2.231e+0
Soil-8	Newton	2.193e-2	1254	3.987e+1	3.906e-2	1.378e+1
	Picard	2.242e-2	610	9.569e+1	7.813e-2	2.833e+1
Soil-9	Newton	5.046e-3	856	6.182e+1	3.125e-1	2.019e+1
	Picard	5.247e-3	448	1.484e+2	6.250e-1	3.857e+1
Soil-10	Newton	1.569e-2	950	5.538e+1	7.813e-2	1.819e+1
	Picard	1.587e-2	525	1.329e+2	1.563e-1	3.291e+1
Soil-11	Newton	2.451e-4	712	7.155e+1	6.250e-1	2.427e+1
	Picard	3.217e-4	465	1.192e+2	1.250e+0	3.716e+1
Soil-12	Newton	Div	Div	Div	Div	Div
	Picard	Div	Div	Div	Div	Div

- *MBE= Mass balance error, Avg.= Average, Div=Divergent.*

Table 3: Computational statistics of the CATHY model for Newton and Picard schemes

Texture	Scheme	NL Ite / Time steps	Lin/ NL	CPU (s)
Soil-1	Newton	5.07	69.90	61909.30
	Picard	6.09	66.90	15772.01
Soil-2	Newton	5.10	53.58	33148.97
	Picard	6.05	52.49	7346.71
Soil-3	Newton	5.37	34.86	11468.41
	Picard	5.53	33.22	2081.05
Soil-4	Newton	5.22	20.43	3873.82
	Picard	5.19	20.94	662.69
Soil-5	Newton	5.04	14.51	1968.74
	Picard	5.04	15.53	363.79
Soil-6	Newton	5.04	17.44	2628.77
	Picard	5.05	18.27	457.70
Soil-7	Newton	5.17	18.86	4896.47
	Picard	4.78	24.65	5333.21
Soil-8	Newton	5.04	14.68	2121.45
	Picard	5.04	15.56	398.27
Soil-9	Newton	5.05	12.24	1381.23
	Picard	5.02	13.53	280.02
Soil-10	Newton	5.05	10.34	1469.22
	Picard	5.04	11.47	312.78
Soil-11	Newton	5.04	10.87	1113.69
	Picard	5.00	12.65	283.46
Soil-12	Newton	Div	Div	Div
	Picard	Div	Div	Div

- *NL=Nonlinear, Ite=Iterations, Lin=Linear*

5.0 Conclusions

The commonly used iterative procedure for solving Richards' equation, the Picard scheme, has been tested in a series of finite element simulations of flow in variably saturated porous media. The examples and numerical results presented demonstrate clearly that the Galerkin finite element formulation developed in this work is effective in handling severely nonlinear cases of variably saturated flow. Various factors affecting the efficiency and robustness of the Picard and Newton methods were investigated and their effects illustrated and summarized in the table and figures for each of the soil texture referred to the Table 1. The most significant features of the present formulation are the Picard algorithm, as well as the scheme is extremely simple to implement and requires very little computational effort in the element matrix evaluation. The iterative

Newton technique is quardatically convergent compared to linear convergence for the Picard method and dynamic time stepping can be easily handled for both the schemes. It has been shown that such procedure can greatly enhance the convergence properties of the iterative solution process as well as the stability of the numerical solution. The numerical results obtained from the algorithm were almost identical for all the soil texture, provided that the same spatial and temporal discretization was employed. Evaluating the scheme for two and three-dimensional flow problem is another important area for future work.

References

Carsel, R.F., Parrish, R.S. (1988). *Developing joint probability distributions of soil water retention characteristic.* Water Resour. Res. 24(5): 755-76.

Celia, M. A. and Binning, P. (1992). *A mass conservative numerical solution for two-phase flow in porous media with application to unsaturated flow*. Water Resour. Res., 28(10): 2819–28.

Cooley, R.L. (1983). *Some new procedures for numerical solution of variably saturated Flow problems.* Water Resour. Res., 19: 1271-1285.

Huyakorn, P. S.; Thomas, S. D. and Thompson, B. M. (1984). *Techniques for making finite elements competitive in modeling flow in variably saturated media*. Water Resources Res., 20: 1099-1115.

Huyakorn, P. S.; Springer, E. P., Guvanasen, V. and Wadsworth, T. D. (1986). *A three dimensional finite element model for simulating water flow in variably saturated porous media*. Water Resources Res., 22: 1790-1808.

Neuman, S. P. (1973). *Saturated-unsaturated seepage by finite elements*. J. Hydraul. Div. ASCE, 99(HY12): 2233-2250.

Paniconi, C. and Putti, M. (1994). *A comparison of Picard and Newton iteration in the numerical solution of multidimensional variably saturated flow problems*. Water Resources Res., 30: 3357–3374.

Paniconi, C., Aldama, A. A. and Wood, E.F. (1991). *Numerical evaluation of iterative and noniterative methods for the solution of the nonlinear Richards equation.* Water Resources Res., 27: 1147-1163.

Pan, L., Wierenga, P.J. (1997). *Improving numerical modeling of two-dimensional water flow in variably saturated, heterogeneous porous media*. Soil. Sci. Soc. Am. J., 61: 335-346.

van Genuchten, M. T., and Nielsen, D. R. (1985). *On describing and predicting the hydraulic properties of unsaturated soils.* Ann. Geophys., 3(5): 615-628.

Vogel, T., van Genuchten, M.T., Cislerova, M. (2011). *Effect of the shape of the soil hydraulic functions near saturation on variably-saturated flow predictions*. Advances in Water Resources, 24:133-144.

Williams, G.A., Miller, C.T., Kelley, C.T. (2000). *Transformation approaches for simulating flow in variably saturated porous media.* Water Resour. Res. 22: 831-840.